Magnetic Materials

DOI: 10.1002/anie.201102048

Ion-Induced Transformation of Magnetism in a Bimetallic CuFe Prussian Blue Analogue**

Masashi Okubo, Daisuke Asakura, Yoshifumi Mizuno, Tetsuichi Kudo, Haoshen Zhou,* Atsushi Okazawa, Norimichi Kojima, Kazumichi Ikedo, Takashi Mizokawa, and Itaru Honma**

In recent decades, the design and synthesis of magnetic porous coordination polymers have attracted considerable attention,[1] because magnetic porous coordination polymers show multiple functionalities, for example, in multiferroic materials and chiral magnets.[2,3] In particular, the switching of magnetism by external stimuli (e.g. light,[4–6] temperature,[7] pressure,[8] and guest molecules[9]) has been actively investigated.

Guest-induced transformation of magnetism using a neutral guest offers perspectives on the correlation of the electronic structure and magnetic properties of porous coordination polymers.[9,10] However, the electrochemical insertion of ionic guests, that is, a pair of an ion and electron, into a porous coordination polymer directly manipulates the electronic structure, and thus the magnetic properties. Therefore, this approach is expected to open new avenues for the design of porous coordination polymers with multifunctionalities. Furthermore, the electrochemical insertion/extraction of ions into/from porous coordination polymers offers the possibility to establish fabrication techniques for novel multifunctional materials, which cannot be obtained by the conventional synthetic methods.

Here, we describe the ion-induced reversible transformation of magnetism in a Prussian blue analogue (PBA). PBA is one of the most studied magnetic coordination polymers and exhibits various magnetic properties because of its strong intermetallic interactions through the bridging CN ligands.[11] Important electrochemical reactions of PBA are the insertion/extraction of various cations (e.g. K^+, Na^+, and Li^+)[12–14] into/from the 3D connected porous structure. Here, we used a bimetallic Fe^{III}-CN-Cu^{II} PBA (CuFe-PBA) as a porous magnetic host, because CuFe-PBA undergoes a ferromagnetic transition at 20 K with a simple spin configuration ($S_{Fe} = 1/2$ and $S_{Cu} = 1/2$).[11] As ionic guests Li ions were used to be inserted/extracted electrochemically.

CuFe-PBA was synthesized by using a precipitation method. The resultant composition of the compound was determined to be $K_{0.14}Cu^{II}_{1.43}[Fe^{III}(CN)_6]\cdot 5H_2O$ by inductively coupled plasma mass spectroscopy for K, Cu, and Fe and a standard microanalytical method for C, H, and N. The powder X-ray diffraction (XRD) pattern (Figure S1a in the Supporting Information) indicated a single cubic phase without impurities, and the calculated lattice parameters ($a = 10.1337(7)$ Å, $V = 1040.7(2)$ Å^3) were consistent with the previously reported values for a bimetallic CuFe-PBA.[15] The mean particle size was estimated to be 40 nm using TEM (Figure S1b in the Supporting Information). The Raman spectrum showed a broad ν(CN) peak centered at 2145 cm^{-1}, which confirmed the valence state of Fe^{III}-CN-Cu^{II}.[15]

Electrochemical insertion and extraction of Li ions were performed by using a three-electrode glass cell, in which the Li metal was employed as counter and reference electrodes. The cutoff voltages were 2.0 V (vs. Li/Li^+) for insertion of Li ions and 4.3 V for extraction of Li ions to prevent the decomposition of CuFe-PBA and the organic solvent.

We used 1M ethylene carbonate/diethyl carbonate solutions of $LiClO_4$ as electrolytes. For our approach, one of the most important requirements is to achieve a homogeneous electronic structure with a uniform concentration of Li ions in the PBA particles. If the Li ion is inserted rapidly, slow diffusion of the Li ions in the solid-solution particles and slow movement at the phase boundary in the phase-separated particles could result in inhomogeneous compounds. Thus, we carried out the electrochemical insertion/extraction of Li ions by repeated application of a low-density current (18 mA g^{-1}) for 10 min, followed by an interruption of 20 min to allow the PBA to equilibrate, that is, we used the galvanostatic intermittent titration technique (GITT).[16] The electrochemical reaction (Scheme 1) is described as given in Equation (1).

$$x\,Li^+ + x\,e^- + K_{0.14}Cu_{1.43}[Fe(CN)_6]\cdot 5H_2O\ (\text{CuFe-PBA}) \rightleftharpoons Li_xK_{0.14}Cu_{1.43}[Fe(CN)_6]\cdot 5H_2O\ (Li_x(\text{CuFe-PBA})) \quad (1)$$

The typical time dependence of the cell voltage and

[*] Dr. M. Okubo, Dr. D. Asakura, Y. Mizuno, Prof. T. Kudo, Dr. H. S. Zhou
National Institute of Advanced Industrial Science and Technology (AIST)
Umezono 1-1-1, Tsukuba, 305-8561 (Japan)
Fax: (+81) 29-861-5648
E-mail: m-okubo@aist.go.jp
hs.zhou@aist.go.jp
Dr. A. Okazawa, Prof. N. Kojima
Graduate School of Arts and Sciences, The University of Tokyo
Komaba 3-8-1, Meguro, Tokyo 153-8902 (Japan)
K. Ikedo, Prof. T. Mizokawa
Department of Complexity Science and Engineering
The University of Tokyo, Kashiwanoha 5-1-5, Chiba 277-8581 (Japan)
Prof. I. Honma
Institute of Multidisciplinary Research for Advanced Materials
Tohoku University, Sendai, Miyagi 980-8577 (Japan)
E-mail: i.honma@tagen.tohoku.ac.jp

[**] This work was financially supported by the Industrial Technology Research Grant Program in 2009 from the New Energy and Industrial Development Organization (NEDO) of Japan.

Supporting information for this article is available on the WWW under http://dx.doi.org/10.1002/anie.201102048.

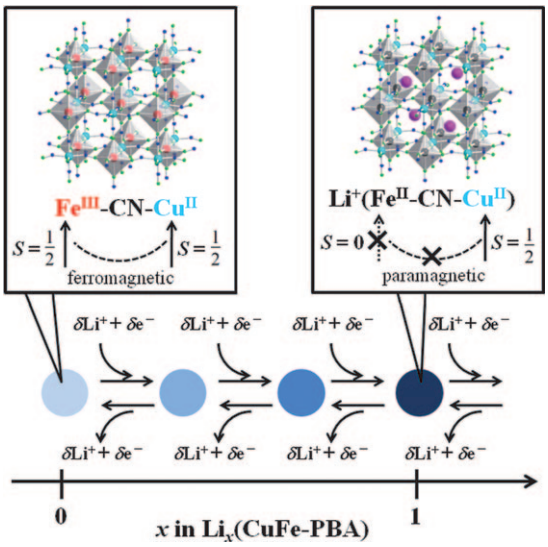

Scheme 1. Electrochemical insertion/extraction of Li ions in the solid-solution state of Li_x(CuFe-PBA) (CuFe-PBA: $K_{0.14}Cu_{1.43}[Fe(CN)_6]\cdot 5H_2O$) and the electronic structure for $x = 0$ and 1.

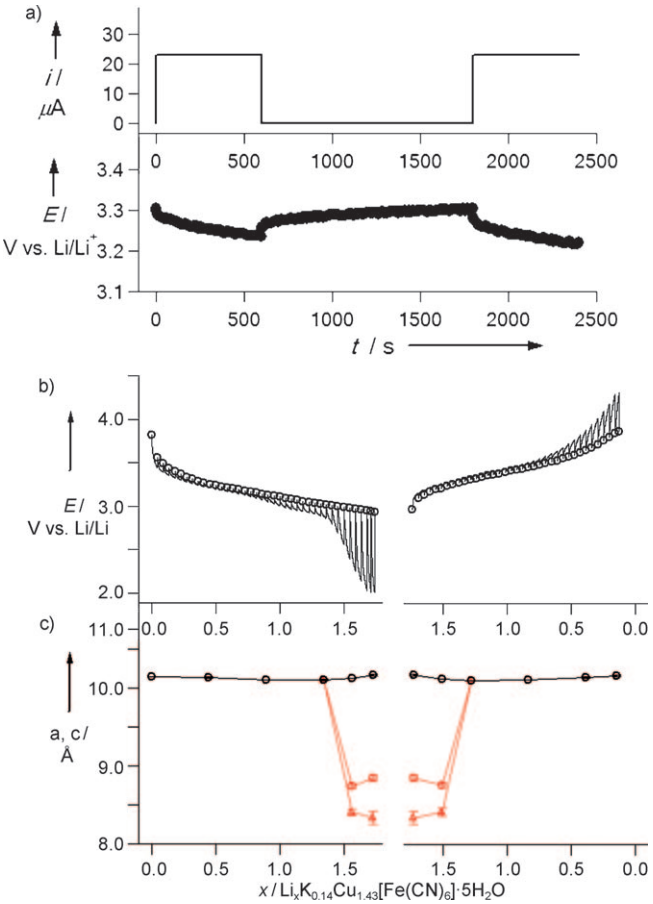

Figure 1. a) Typical time (t) dependence of the cell voltage (E) and current (i) during the insertion of Li ions by the GITT. b) Equilibrium voltage as a function of x for Li_xCuFe (empty circles). The left-hand side shows insertion and the right-hand side shows extraction of Li ions. The solid line displays the change in voltage of the electrochemical cell at a constant current. c) Unit-cell parameters as a function of x. Black empty circles (a_{cubic}) denote the cell parameter for the cubic phase, red empty circles ($\sqrt{2}a_{tetragonal}$) and red empty triangles ($c_{tetragonal}$) denote the cell parameters for the tetragonal phase.

applied current measured by the GITT experiment is shown in Figure 1 a. The electric current used for the insertion of Li ions gradually decreased the cell voltage because of the gradual increase in the concentration of Li ions at the surface. Then, the 20 min interruption allowed the CuFe-PBA particle to equilibrate at a uniform concentration of Li ions.

Figure 1 b shows the equilibrium voltage (empty circles) as a function of x for Li_x(CuFe-PBA). The solid line in Figure 1 b displays the change in voltage during the GITT experiment. The equilibrium voltage shows that the insertion/extraction of Li ions occurs between 3.5 and 3.0 V measured versus the Li/Li^+ electrode. The amount x of inserted Li ions reached 1.75 and exceeded the amount of Fe^{II} obtained from the redox reaction of Fe^{III} to Fe^{II}. Furthermore, the inserted Li ions were extracted nearly reversibly. This result suggests that the insertion of Li ions in CuFe-PBA was accompanied by a reversible redox reaction of both Fe and Cu ions.

To clarify the structural changes observed during the insertion/extraction of Li ions, ex situ XRD patterns were recorded for Li_x(CuFe-PBA) (see Figure S2 in the Supporting Information). Figure 1 c shows the lattice parameters as a function of x. For all compounds with $x < 1.34$, the lattice parameter a monotonically decreased from 10.1337(7) ($x = 0$) to 10.101(6) Å ($x = 1.34$). This result suggests that the insertion/extraction of Li ions for $x < 1.34$ occurs in the solid-solution state, in which the concentration of Li ions x changes continuously within the PBA particles. Scheme 1 illustrates the electrochemical insertion/extraction of Li ions in CuFe-PBA. However, for compounds with $x > 1.34$, the intensity of the cubic phase gradually decreased and new peaks of a tetragonal phase emerged. The emerging tetragonal phase disappeared and was transformed into the cubic phase when the Li ions were extracted. Therefore, the tetragonal phase cannot be ascribed to a product, resulting from the decomposition of CuFe-PBA, but to CuFe-PBA with a high concentration of Li ions. This result clearly suggests phase separation in Li-rich and Li-poor phases, and the insertion/extraction of Li ions occurs as a fractional change in the volume of the two phases.

In general, the two phase states show a flat voltage plateau (non-Nernst type curve) for the insertion/extraction of Li ions (e.g., $LiFePO_4$ displays a flat voltage plateau at 3.5 V.[17]) However, for the two phase states of Li_x(CuFe-PBA) with $x > 1.34$ we observed rather a sloping profile (Figure 1 b) instead of a flat plateau. One possible explanation for our observation is a short relaxation time in the GITT experiment. The 20 min interruption may be too short for the PBA to equilibrate. However, this sloping profile can also be explained by the small particle size of CuFe-PBA. As shown in the TEM images (Figure S1B in the Supporting Information), the mean particle size is about 40 nm. As reported frequently, nano-sized electrode materials show a sloping voltage profile even in both phase states.[18] Nevertheless, to avoid the necessity of phase separation, we focused on the magnetism of Li_x(CuFe-PBA) with $0 < x < 1$.

We performed magnetic measurements using three samples: CuFe-PBA before (CuFe-PBA) and after insertion of Li ions (Li_1(CuFe-PBA)) as well as after insertion/extraction of Li ions (Li_0(CuFe-PBA)). The value of χT (χ = magnetic susceptibility) at room temperature for CuFe-PBA was 1.33 emu K mol^{-1} (see Figure S3 in the Supporting Information), which was slightly higher than the spin-only value (0.91 emu K mol^{-1}). The slight discrepancy between the experimental and spin-only values can be ascribed to the contribution from the orbital angular momentum of low-spin Fe^{III} ions. With decreasing temperature the χT value increased monotonically at a Weiss constant θ of 19.9 K; this increase indicates a ferromagnetic interaction between Cu^{II} and Fe^{III} ions. Figure 2a shows the field-cooled magnetization M of CuFe-PBA. The remarkable increase in M below 20 K suggests a ferromagnetic transition at $T_C = 20$ K. As the ratio of θ and T_C is almost unity, the magnetic interaction from second-nearest neighbors (Fe^{III}–Fe^{III} and Cu^{II}–Cu^{II}) is negligible according to molecular field theory.[19] The M–H curve at 2 K (Figure 2b) displays a large hysteresis loop with a coercive field (H_{cr}) of 2740 Oe and a residual magnetization (M_r) of 7200 emu Oe mol^{-1}.

In contrast, the magnetic properties were significantly altered by the insertion of Li ions. The value of χT at room temperature decreased to 0.94 emu K mol^{-1} by insertion of Li ions (see Figure S3 in the Supporting Information), and this value remained nearly constant with decreasing temperature. Furthermore, the field-cooled magnetization of Li_1(CuFe-PBA) measured from 40 to 2 K did not increase (Figure 2a), and the M–H curve at 2 K did not show a hysteresis loop, which indicates the disappearance of the ferromagnetic transition.

To confirm the change in the electronic structure, we measured ^{57}Fe Mössbauer and XPS spectra of CuFe-PBA and Li_1(CuFe-PBA) (Figure 3). The black dots in Figure 3a were obtained by ^{57}Fe Mössbauer spectroscopy, and the solid lines are fitted curves. The spectrum of CuFe-PBA showed a broad

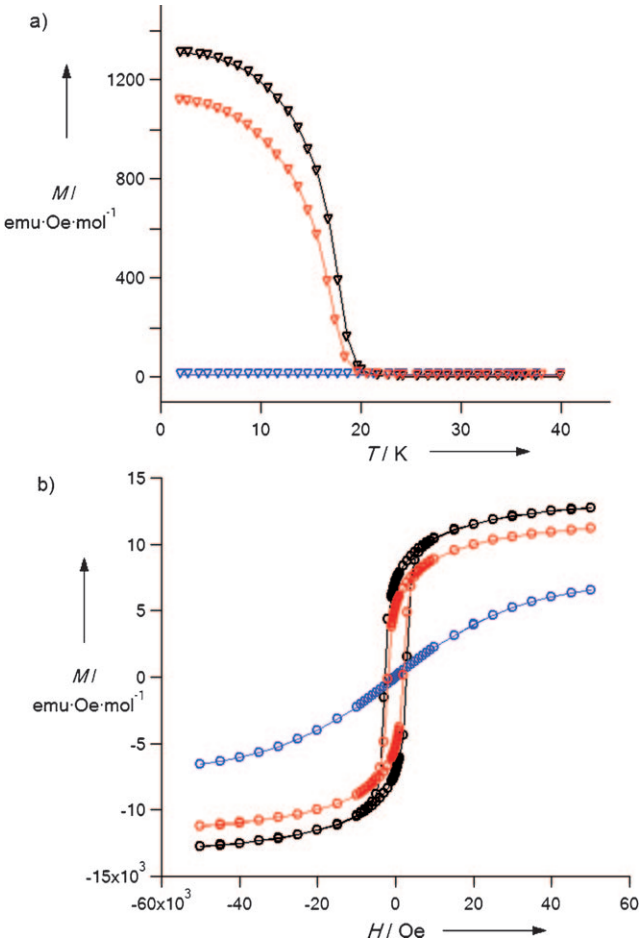

Figure 2. a) Field-cooled magnetization at 10 Oe, and b) M–H curve at 2 K for Li_x(CuFe-PBA). Black, blue, and red points are magnetization values for CuFe-PBA, Li_1(CuFe-PBA), and Li_0(CuFe-PBA), respectively.

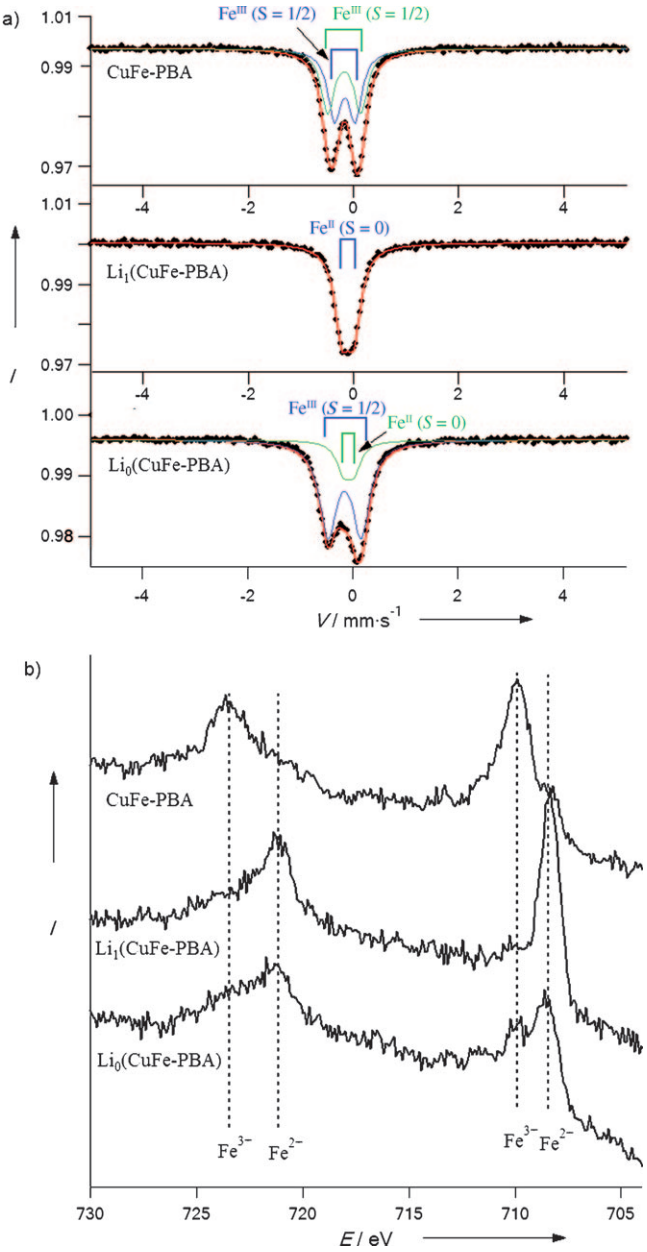

Figure 3. a) Mössbauer (black dots: experimental data, solid lines: fitted curves), and b) Fe 2p XPS spectra for CuFe-PBA, Li_1(CuFe-PBA), and Li_0(CuFe-PBA).

doublet, and the best-fitted curve required two doublets (blue and green solid lines). The fitting parameters are summarized in Table S1 in the Supporting Information. Both doublets have almost typical values of an isomer shift (IS) and a quadrupole splitting (QS) for an octahedral low-spin Fe^{III} ion as in $[Fe^{III}(CN)_6]^{3-}$ ($IS = -0.12\ mm\,s^{-1}$, $QS = 0.28\ mm\,s^{-1}$).[20] The broad line shape generally suggests a disordered coordination environment of Fe. As CuFe-PBA contains a large amount of $[Fe(CN)_6]$ vacancies, the broad line shape may be a result of the disordered coordination environment induced by the $[Fe(CN)_6]$ vacancies. The Fe 2p core-level XPS signals in CuFe-PBA at 710 and 723.5 eV correspond to Fe^{III} $2p_{3/2}$ and $2p_{1/2}$, respectively.[14] This observation agrees well with the Mössbauer results. In contrast, after insertion of Li ions, the Mössbauer spectrum for Li_1(CuFe-PBA) showed a broad singlet, which is fitted by a slightly splitted doublet. The obtained IS and QS values (see Table S1 in the Supporting Information) are consistent with the previously reported values for an octahedral low-spin Fe^{II} ion in $[Fe^{II}(CN)_6]^{4-}$ ($IS = -0.05\ mm\,s^{-1}$, $QS = 0\ mm\,s^{-1}$).[20] These results clearly proved that Fe^{III} is completely reduced to Fe^{II} by insertion of Li ions and confirm the spin-state transformation from Fe^{III} ($S_{Fe} = 1/2$) to Fe^{II} ($S_{Fe} = 0$) by insertion of Li ions (Scheme 1). After insertion of Li ions, the Fe 2p core-level XPS signals of Li_1(CuFe-PBA) are shifted from 710 to 708 eV ($2p_{3/2}$) and from 723.5 to 721 eV ($2p_{1/2}$), respectively. This observation also confirmed the complete reduction of Fe^{III} to Fe^{II} by insertion of Li ions.

The complete transformation from a ferromagnet to a paramagnet by guest ions is very rare, although variations in the magnetic properties caused by electrochemical processes have long been regarded as diagnostic of the redox state of the transition-metal ions. The magnetic transition in typical magnetic electrodes like oxides (e.g. Li_xCrO_2[21]) is difficult to eliminate because of strong magnetic interactions. In contrast, if magnetic interactions from second-nearest neighbors are negligible, the reduction of Fe^{III} to Fe^{II} in, for example, CuFe-PBA is sufficient to eliminate the magnetic transition.

When the Li guest ions were extracted, Li_0(CuFe-PBA) recovered the magnetic behavior resulting from ferromagnetic interactions. The value of χT at room temperature was increased to $1.30\ emu\,K\,mol^{-1}$ by extraction of Li ions (see Figure S3 in the Supporting Information), and it increased at a Weiss constant of 16.4 K with decreasing temperature. The field-cooled magnetization again showed a rapid increase at 19.5 K. The *M*–*H* curve at 2 K displays a hysteresis loop with $H_{cr} = 1960$ Oe and $M_r = 5300\ emu\,Oe\,mol^{-1}$. This finding suggests that the Fe ions were oxidized and the ferromagnetic interaction between Fe and Cu ions was recovered.

Finally, the switching of magnetism is reversibile. Comparision of the field-cooled magnetization and saturation magnetization curves of CuFe-PBA and Li_0(CuFe-PBA) (Figure 2b) shows a slight decrease ($\approx 15\%$) after the first insertion/extraction cycle of Li ions. The ^{57}Fe Mössbauer spectrum of Li_0(CuFe-PBA) was best-fitted by a major doublet (blue line for low-spin Fe^{III} in Figure 3a) and a minor slightly splitted doublet (green line for low-spin Fe^{II}). This result indicated that 20% of the Fe is in the valence state of Fe^{II} even after extraction of the Li ions at a cutoff voltage of 4.3 V.

According to the molecular field theory,[19] the ferromagnetic transition temperature T_C for the bimetallic CuFe-PBA is given in Equation (2),

$$T_C = \frac{2|J|}{3k}\sqrt{Z_{Cu Fe^{III}} Z_{Fe^{III} Cu}}\sqrt{S_{Cu}(S_{Cu}+1)}\sqrt{S_{Fe^{III}}(S_{Fe^{III}}+1)} \quad (2)$$

where Z_{ij} is the number of nearest-neighbor sites *i* surrounding sites *j*, *J* is the superexchange constant between Fe^{III} and Cu^{II}, *k* is the Boltzmann constant, and S_i is the spin of the site *i*. When 20% of the diamagnetic Fe^{II} ($S = 0$) is distributed homogeneously within the Li_0(CuFe-PBA) particle and *J* is assumed to be constant, T_C is expected to decrease to 17.9 K, which is lower than the experimental result ($T_C = 19.5$ K). This discrepancy indicates that the diamagnetic Fe^{II} locates rather heterogeneously. Since the surface-sensitive XPS spectrum of Li_0(CuFe-PBA) showed a larger fraction of Fe^{II} than do ^{57}Fe Mössbauer spectra, most Fe^{II} ions should locate near the surface. Most likely, the electrochemical side-reactions at the surface may induce the redox-inactive and diamagnetic Fe^{II} ions, resulting in the degradation of the magnetization value. However, as shown in Figure S4 in the Supporting Information, switching between ferromagnetism and paramagnetism is reversible for five cycles.

In summary, the magnetism in the bimetallic CuFe-PBA was reversibly switched between ferromagnetism and paramagnetism by insertion/extraction of Li guest ions. These results provide insight into the manipulation of the electronic structure of porous coordination polymers and propose a fabrication method for novel multifunctional porous coordination magnets.

Experimental Section

CuFe-PBA was synthesized by using a precipitation method. Typically, an aqueous solution of $CuSO_4{\cdot}5H_2O$ was added dropwise to an aqueous solution of $K_3[Fe(CN)_6]$. The precipitate was centrifuged, washed with distilled water, and then dried in vacuum for 24 h. The obtained products were stored under an inert atmosphere in the dark at 5 °C to prevent decomposition.

Elemental analysis calcd (%) for $K_{0.14}Cu_{1.43}[Fe(CN)_6]{\cdot}5H_2O$: K 1.37, Cu 22.81, Fe 14.02, C 18.09, N 21.10, H 2.54; found: K 1.48, Cu 21.9, Fe 13.4, C 18.20, N 19.86, H 2.62. Raman (excitation: 632.8 nm): 2145 cm^{-1} (ν_{CN}).

Raman spectra were obtained by using a Nihon Bunko Ventuno spectrometer (NSR-1000DT) at room temperature in backward geometry. The powder samples were excited at a wavelength of 632.8 nm by a He–Ne laser. Powder XRD measurements were conducted using a Bruker D8 Advance spectrometer with $Cu_{K\alpha}$ radiation in steps of 0.008° over the 2θ range from 5 to 80°. The unit cell parameters were calculated by least-square fitting. Ex situ XRD patterns were recorded after washing the lithium-inserted/extracted (in the GITT mode) samples with ethanol.

For electrochemical measurements, each sample (50 mg) was ground into a paste with acetylene black (13.3 mg) and poly(tetrafluoroethylene) (3.3 mg). Lithium metal was used as the counter and reference electrodes, and 1M ethylene carbonate (EC)/diethyl carbonate (DEC) solutions of $LiClO_4$ were used as electrolytes. The cutoff voltages were 4.3 V for charge (extraction of Li ions) and 2.0 V for discharge (insertion of Li ions). The open circuit voltage (OCV)

was recorded by using the galvanostatic intermittent titration technique (GITT) with repetition of slow charge/discharge at 18 mA g^{-1} for 10 min, followed by an interruption for 20 min. A slight discrepancy between the amount of inserted Li ions and the electrochemical capacity may be possible, when K ions in the PBA samples are extracted. However, the amount of K ions in the PBA samples is so small that it can be ignored in this study.

The direct current (DC) magnetic susceptibility was measured on a Quantum Design MPMS5S SQUID susceptometer. The magnetic susceptibility was corrected for core diamagnetism estimated from the Pascal constants and Pauli paramagnetism because of the used acetylene black. For ^{57}Fe Mössbauer spectroscopy, ^{57}Co in Rh was used as Mössbauer source. The spectra were calibrated by using six lines of α-Fe, the center of which was taken as zero isomer shift. The XPS measurements were carried out at room temperature using a JEOL JPS-9200 hemispherical analyzer and $Al_{K\alpha}$ source ($h\nu$ = 1486.6 eV).

Received: March 23, 2011
Published online: May 25, 2011

Keywords: coordination chemistry · electrochemistry · electronic structure · magnetic materials · Mössbauer spectroscopy

[1] *Magnetism: Molecules to Materials* (Eds.: J. S. Miller, M. Drillon), Wiley-VCH, Berlin, **2001**.
[2] S. Ohkoshi, H. Tokoro, T. Matsuda, H. Takahashi, H. Irie, K. Hashimoto, *Angew. Chem.* **2007**, *119*, 3302; *Angew. Chem. Int. Ed.* **2007**, *46*, 3238.
[3] C. Train, R. Gheorghe, V. Krstic, L.-M. Chamoreau, N. S. Ovanesyan, G. L. J. A. Rikken, M. Gruselle, M. Verdaguer, *Nat. Mater.* **2008**, *7*, 729.
[4] O. Sato, T. Iyoda, A. Fujishima, K. Hashimoto, *Science* **1996**, *272*, 704.
[5] N. Kida, M. Hikita, I. Kashima, M. Okubo, M. Itoi, M. Enomoto, K. Kato, M. Takata, N. Kojima, *J. Am. Chem. Soc.* **2009**, *131*, 212–220.
[6] M. Okubo, M. Enomoto, N. Kojima, *Solid State Commun.* **2005**, *134*, 777.
[7] S. Ohkoshi, T. Matsuda, H. Tokoro, K. Hashimoto, *Chem. Mater.* **2005**, *17*, 81.
[8] E. Coronado, M. C. Jimenez-Lopez, T. Korzeniak, G. Levchenko, F. M. Romero, A. Segura, V. Garcia-Baonza, J. C. Cezar, F. M. F. de Groot, A. Milner, M. Paz-Pasternak, *J. Am. Chem. Soc.* **2008**, *130*, 15519.
[9] B. Li, R. J. Wei, R. B. Huang, L. S. Zheng, Z. Zheng, *J. Am. Chem. Soc.* **2010**, *132*, 1558.
[10] S. M. Neville, G. J. Halder, K. W. Chapman, M. B. Duriska, B. Moubaraki, K. S. Murray, C. J. Kepert, *J. Am. Chem. Soc.* **2009**, *131*, 12106.
[11] M. Verdaguer, G. S. Girolami, *Magnetic Prussian blue analogs* in *Magnetism: Molecules to Materials V* (Eds.: J. S. Miller, M. Dorillon), Wiley-VCH, New York, **2005**.
[12] K. Itaya, I. Uchida, V. D. Neff, *Acc. Chem. Res.* **1986**, *19*, 162.
[13] N. R. de Tacconi, K. Rajeshwar, *Chem. Mater.* **2003**, *15*, 3046.
[14] M. Okubo, D. Asakura, Y. Mizuno, J. D. Kim, T. Mizokawa, T. Kudo, I. Honma, *J. Phys. Chem. Lett.* **2010**, *1*, 2063.
[15] E. Reguera, J. Rodriguez-Hernandez, A. Champi, J. G. Duque, E. Granado, C. Z. Z. Rettori, *Z. Phys. Chem.* **2006**, *220*, 1609.
[16] W. Weppner, R. A. Huggins, *J. Electrochem. Soc.* **1977**, *124*, 1569.
[17] E. Hosono, Y. G. Wang, N. Kida, M. Enomoto, N. Kojima, M. Okubo, H. Matsuda, Y. Saito, T. Kudo, I. Honma, H. S. Zhou, *ACS Appl. Mater. Interfaces* **2010**, *2*, 212.
[18] M. Okubo, Y. Mizuno, H. Yamada, J. D. Kim, E. Hosono, H. S. Zhou, T. Kudo, I. Honma, *ACS Nano* **2010**, *4*, 741.
[19] L. Néel, *Ann. Phys.* **1948**, *3*, 137.
[20] N. N. Greenwood, T. C. Gibb, *Mössbauer spectroscopy*m Capman&Hall, London, **1971**.
[21] V. Sivakumar, C. A. Ross, N. Yabuuchi, Y. Shao-Horn, K. Persson, G. Ceder, *J. Electrochem. Soc.* **2008**, *155*, P83.

